

Observation of the Doubly Cabibbo-Suppressed Decay $D^+ \rightarrow K^+\pi^+\pi^-\pi^0$ and Evidence for $D^+ \rightarrow K^+\omega$

M. Ablikim¹, M. N. Achasov^{10,c}, P. Adlarson⁶⁴, S. Ahmed¹⁵, M. Albrecht⁴, A. Amoroso^{63A,63C}, Q. An^{60,48}, Anita²¹, X. H. Bai⁵⁴, Y. Bai⁴⁷, O. Bakina²⁹, R. Baldini Ferroli^{23A}, I. Balossino^{24A}, Y. Ban^{38,k}, K. Begzsuren²⁶, J. V. Bennett⁵, N. Berger²⁸, M. Bertani^{23A}, D. Bettoni^{24A}, F. Bianchi^{63A,63C}, J. Biernat⁶⁴, J. Bloms⁵⁷, A. Bortone^{63A,63C}, I. Boyko²⁹, R. A. Briere⁵, H. Cai⁶⁵, X. Cai^{1,48}, A. Calcaterra^{23A}, G. F. Cao^{1,52}, N. Cao^{1,52}, S. A. Cetin^{51B}, J. F. Chang^{1,48}, W. L. Chang^{1,52}, G. Chelkov^{29,b}, D. Y. Chen⁶, G. Chen¹, H. S. Chen^{1,52}, M. L. Chen^{1,48}, S. J. Chen³⁶, X. R. Chen²⁵, Y. B. Chen^{1,48}, Z. J. Chen^{20,l}, W. S. Cheng^{63C}, G. Cibinetto^{24A}, F. Cossio^{63C}, X. F. Cui³⁷, H. L. Dai^{1,48}, J. P. Dai^{42,g}, X. C. Dai^{1,52}, A. Dbeyssi¹⁵, R. B. de Boer⁴, D. Dedovich²⁹, Z. Y. Deng¹, A. Denig²⁸, I. Denysenko²⁹, M. Destefanis^{63A,63C}, F. De Mori^{63A,63C}, Y. Ding³⁴, C. Dong³⁷, J. Dong^{1,48}, L. Y. Dong^{1,52}, M. Y. Dong^{1,48,52}, S. X. Du⁶⁸, J. Fang^{1,48}, S. S. Fang^{1,52}, Y. Fang¹, R. Farinelli^{24A}, L. Fava^{63B,63C}, F. Feldbauer⁴, G. Felici^{23A}, C. Q. Feng^{60,48}, M. Fritsch⁴, C. D. Fu¹, Y. Fu¹, X. L. Gao^{60,48}, Y. Gao⁶¹, Y. Gao^{38,k}, Y. G. Gao⁶, I. Garzia^{24A,24B}, E. M. Gersabeck⁵⁵, A. Gilman⁵⁶, K. Goetzen¹¹, L. Gong³⁷, W. X. Gong^{1,48}, W. Gradl²⁸, M. Greco^{63A,63C}, L. M. Gu³⁶, M. H. Gu^{1,48}, S. Gu², Y. T. Gu¹³, C. Y. Guan^{1,52}, A. Q. Guo²², L. B. Guo³⁵, R. P. Guo⁴⁰, Y. P. Guo²⁸, Y. P. Guo^{9,h}, A. Guskov²⁹, S. Han⁶⁵, T. T. Han⁴¹, T. Z. Han^{9,h}, X. Q. Hao¹⁶, F. A. Harris⁵³, K. L. He^{1,52}, F. H. Heinsius⁴, T. Held⁴, Y. K. Heng^{1,48,52}, M. Himmelreich^{11,f}, T. Holtmann⁴, Y. R. Hou⁵², Z. L. Hou¹, H. M. Hu^{1,52}, J. F. Hu^{42,g}, T. Hu^{1,48,52}, Y. Hu¹, G. S. Huang^{60,48}, L. Q. Huang⁶¹, X. T. Huang⁴¹, Y. P. Huang¹, Z. Huang^{38,k}, N. Huesken⁵⁷, T. Hussain⁶², W. Ikegami Andersson⁶⁴, W. Imoehl²², M. Irshad^{60,48}, S. Jaeger⁴, S. Janchiv^{26,j}, Q. Ji¹, Q. P. Ji¹⁶, X. B. Ji^{1,52}, X. L. Ji^{1,48}, H. B. Jiang⁴¹, X. S. Jiang^{1,48,52}, X. Y. Jiang³⁷, J. B. Jiao⁴¹, Z. Jiao¹⁸, S. Jin³⁶, Y. Jin⁵⁴, T. Johansson⁶⁴, N. Kalantar-Nayestanaki³¹, X. S. Kang³⁴, R. Kappert³¹, M. Kavatsyuk³¹, B. C. Ke^{43,1}, I. K. Keshk⁴, A. Khoukaz⁵⁷, P. Kiese²⁸, R. Kiuchi¹, R. Kliemt¹¹, L. Koch³⁰, O. B. Kolcu^{51B,e}, B. Kopf⁴, M. Kuemmel⁴, M. Kuessner⁴, A. Kupsc⁶⁴, M. G. Kurth^{1,52}, W. Kühn³⁰, J. J. Lane⁵⁵, J. S. Lange³⁰, P. Larin¹⁵, L. Lavezzi^{63A,63C}, H. Leithoff²⁸, M. Lellmann²⁸, T. Lenz²⁸, C. Li³⁹, C. H. Li³³, Cheng Li^{60,48}, D. M. Li⁶⁸, F. Li^{1,48}, G. Li¹, H. B. Li^{1,52}, H. J. Li^{9,h}, J. L. Li⁴¹, J. Q. Li⁴, Ke Li¹, L. K. Li¹, Lei Li³, P. L. Li^{60,48}, P. R. Li³², S. Y. Li⁵⁰, W. D. Li^{1,52}, W. G. Li¹, X. H. Li^{60,48}, X. L. Li⁴¹, Z. B. Li⁴⁹, Z. Y. Li⁴⁹, H. Liang^{1,52}, H. Liang^{60,48}, Y. F. Liang⁴⁵, Y. T. Liang²⁵, L. Z. Liao^{1,52}, J. Libby²¹, C. X. Lin⁴⁹, B. Liu^{42,g}, B. J. Liu¹, C. X. Liu¹, D. Liu^{60,48}, D. Y. Liu^{42,g}, F. H. Liu⁴⁴, Fang Liu¹, Feng Liu⁶, H. B. Liu¹³, H. M. Liu^{1,52}, Huanhuan Liu¹, Huihui Liu¹⁷, J. B. Liu^{60,48}, J. Y. Liu^{1,52}, K. Liu¹, K. Y. Liu³⁴, Ke Liu⁶, L. Liu^{60,48}, Q. Liu⁵², S. B. Liu^{60,48}, Shuai Liu⁴⁶, T. Liu^{1,52}, X. Liu³², Y. B. Liu³⁷, Z. A. Liu^{1,48,52}, Z. Q. Liu⁴¹, Y. F. Long^{38,k}, X. C. Lou^{1,48,52}, F. X. Lu¹⁶, H. J. Lu¹⁸, J. D. Lu^{1,52}, J. G. Lu^{1,48}, X. L. Lu¹, Y. Lu¹, Y. P. Lu^{1,48}, C. L. Luo³⁵, M. X. Luo⁶⁷, P. W. Luo⁴⁹, T. Luo^{9,h}, X. L. Luo^{1,48}, S. Lusso^{63C}, X. R. Lyu⁵², F. C. Ma³⁴, H. L. Ma¹, L. L. Ma⁴¹, M. M. Ma^{1,52}, Q. M. Ma¹, R. Q. Ma^{1,52}, R. T. Ma⁵², X. N. Ma³⁷, X. X. Ma^{1,52}, X. Y. Ma^{1,48}, Y. M. Ma⁴¹, F. E. Maas¹⁵, M. Maggiora^{63A,63C}, S. Maldaner²⁸, S. Malde⁵⁸, Q. A. Malik⁶², A. Mangoni^{23B}, Y. J. Mao^{38,k}, Z. P. Mao¹, S. Marcello^{63A,63C}, Z. X. Meng⁵⁴, J. G. Messchendorp³¹, G. Mezzadri^{24A}, T. J. Min³⁶, R. E. Mitchell²², X. H. Mo^{1,48,52}, Y. J. Mo⁶, N. Yu. Muchnoi^{10,c}, H. Muramatsu⁵⁶, S. Nakhoul^{11,f}, Y. Nefedov²⁹, F. Nerling^{11,f}, I. B. Nikolaev^{10,c}, Z. Ning^{1,48}, S. Nisar^{8,i}, S. L. Olsen⁵², Q. Ouyang^{1,48,52}, S. Pacetti^{23B,23C}, X. Pan^{9,h}, Y. Pan⁵⁵, A. Pathak¹, P. Patteri^{23A}, M. Pelizaeus⁴, H. P. Peng^{60,48}, K. Peters^{11,f}, J. Pettersson⁶⁴, J. L. Ping³⁵, R. G. Ping^{1,52}, A. Pitka⁴, R. Poling⁵⁶, V. Prasad^{60,48}, H. Qi^{60,48}, H. R. Qi⁵⁰, M. Qi³⁶, T. Y. Qi², T. Y. Qi⁹, S. Qian^{1,48}, W.-B. Qian⁵², Z. Qian⁴⁹, C. F. Qiao⁵², L. Q. Qin¹², X. S. Qin⁴, Z. H. Qin^{1,48}, J. F. Qiu¹, S. Q. Qu³⁷, K. H. Rashid⁶², K. Ravindran²¹, C. F. Redmer²⁸, A. Rivetti^{63C}, V. Rodin³¹, M. Rolo^{63C}, G. Rong^{1,52}, Ch. Rosner¹⁵, M. Rump⁵⁷, A. Sarantsev^{29,d}, Y. Schelhaas²⁸, C. Schnier⁴, K. Schoenning⁶⁴, D. C. Shan⁴⁶, W. Shan¹⁹, X. Y. Shan^{60,48}, M. Shao^{60,48}, C. P. Shen⁹, P. X. Shen³⁷, X. Y. Shen^{1,52}, H. C. Shi^{60,48}, R. S. Shi^{1,52}, X. Shi^{1,48}, X. D. Shi^{60,48}, J. J. Song⁴¹, Q. Q. Song^{60,48}, W. M. Song^{27,1}, Y. X. Song^{38,k}, S. Sosio^{63A,63C}, S. Spataro^{63A,63C}, F. F. Sui⁴¹, G. X. Sun¹, J. F. Sun¹⁶, L. Sun⁶⁵, S. S. Sun^{1,52}, T. Sun^{1,52}, W. Y. Sun³⁵, X. Sun^{20,l}, Y. J. Sun^{60,48}, Y. K. Sun^{60,48}, Y. Z. Sun¹, Z. T. Sun¹, Y. H. Tan⁶⁵, Y. X. Tan^{60,48}, C. J. Tang⁴⁵, G. Y. Tang¹, J. Tang⁴⁹, V. Thoren⁶⁴, I. Uman^{51D}, B. Wang¹, B. L. Wang⁵², C. W. Wang³⁶, D. Y. Wang^{38,k}, H. P. Wang^{1,52}, K. Wang^{1,48}, L. L. Wang¹, M. Wang⁴¹, M. Z. Wang^{38,k}, Meng Wang^{1,52}, W. H. Wang⁶⁵, W. P. Wang^{60,48}, X. Wang^{38,k}, X. F. Wang³², X. L. Wang^{9,h}, Y. Wang⁴⁹, Y. Wang^{60,48}, Y. D. Wang¹⁵, Y. F. Wang^{1,48,52}, Y. Q. Wang¹, Z. Wang^{1,48}, Z. Y. Wang¹, Ziyi Wang⁵², Zongyuan Wang^{1,52}, D. H. Wei¹², P. Weidenkaff²⁸, F. Weidner⁵⁷, S. P. Wen¹, D. J. White⁵⁵, U. Wiedner⁴,

G. Wilkinson⁵⁸, M. Wolke⁶⁴, L. Wollenberg⁴, J. F. Wu^{1,52}, L. H. Wu¹, L. J. Wu^{1,52}, X. Wu^{9,h}, Z. Wu^{1,48}, L. Xia^{60,48}, H. Xiao^{9,h}, S. Y. Xiao¹, Y. J. Xiao^{1,52}, Z. J. Xiao³⁵, X. H. Xie^{38,k}, Y. G. Xie^{1,48}, Y. H. Xie⁶, T. Y. Xing^{1,52}, X. A. Xiong^{1,52}, G. F. Xu¹, J. J. Xu³⁶, Q. J. Xu¹⁴, W. Xu^{1,52}, X. P. Xu⁴⁶, F. Yan^{9,h}, L. Yan^{63A,63C}, L. Yan^{9,h}, W. B. Yan^{60,48}, W. C. Yan⁶⁸, Xu Yan⁴⁶, H. J. Yang^{42,g}, H. X. Yang¹, L. Yang⁶⁵, R. X. Yang^{60,48}, S. L. Yang^{1,52}, Y. H. Yang³⁶, Y. X. Yang¹², Yifan Yang^{1,52}, Zhi Yang²⁵, M. Ye^{1,48}, M. H. Ye⁷, J. H. Yin¹, Z. Y. You⁴⁹, B. X. Yu^{1,48,52}, C. X. Yu³⁷, G. Yu^{1,52}, J. S. Yu^{20,l}, T. Yu⁶¹, C. Z. Yuan^{1,52}, W. Yuan^{63A,63C}, X. Q. Yuan^{38,k}, Y. Yuan¹, Z. Y. Yuan⁴⁹, C. X. Yue³³, A. Yuncu^{51B,a}, A. A. Zafar⁶², Y. Zeng^{20,l}, B. X. Zhang¹, Guangyi Zhang¹⁶, H. H. Zhang⁴⁹, H. Y. Zhang^{1,48}, J. L. Zhang⁶⁶, J. Q. Zhang⁴, J. W. Zhang^{1,48,52}, J. Y. Zhang¹, J. Z. Zhang^{1,52}, Jianyu Zhang^{1,52}, Jiawei Zhang^{1,52}, L. Zhang¹, Lei Zhang³⁶, S. Zhang⁴⁹, S. F. Zhang³⁶, T. J. Zhang^{42,g}, X. Y. Zhang⁴¹, Y. Zhang⁵⁸, Y. H. Zhang^{1,48}, Y. T. Zhang^{60,48}, Yan Zhang^{60,48}, Yao Zhang¹, Yi Zhang^{9,h}, Z. H. Zhang⁶, Z. Y. Zhang⁶⁵, G. Zhao¹, J. Zhao³³, J. Y. Zhao^{1,52}, J. Z. Zhao^{1,48}, Lei Zhao^{60,48}, Ling Zhao¹, M. G. Zhao³⁷, Q. Zhao¹, S. J. Zhao⁶⁸, Y. B. Zhao^{1,48}, Y. X. Zhao²⁵, Z. G. Zhao^{60,48}, A. Zhemchugov^{29,b}, B. Zheng⁶¹, J. P. Zheng^{1,48}, Y. Zheng^{38,k}, Y. H. Zheng⁵², B. Zhong³⁵, C. Zhong⁶¹, L. P. Zhou^{1,52}, Q. Zhou^{1,52}, X. Zhou⁶⁵, X. K. Zhou⁵², X. R. Zhou^{60,48}, A. N. Zhu^{1,52}, J. Zhu³⁷, K. Zhu¹, K. J. Zhu^{1,48,52}, S. H. Zhu⁵⁹, W. J. Zhu³⁷, X. L. Zhu⁵⁰, Y. C. Zhu^{60,48}, Z. A. Zhu^{1,52}, B. S. Zou¹, J. H. Zou¹

(BESIII Collaboration)

¹ *Institute of High Energy Physics, Beijing 100049, People's Republic of China*

² *Beihang University, Beijing 100191, People's Republic of China*

³ *Beijing Institute of Petrochemical Technology, Beijing 102617, People's Republic of China*

⁴ *Bochum Ruhr-University, D-44780 Bochum, Germany*

⁵ *Carnegie Mellon University, Pittsburgh, Pennsylvania 15213, USA*

⁶ *Central China Normal University, Wuhan 430079, People's Republic of China*

⁷ *China Center of Advanced Science and Technology, Beijing 100190, People's Republic of China*

⁸ *COMSATS University Islamabad, Lahore Campus, Defence Road, Off Raiwind Road, 54000 Lahore, Pakistan*

⁹ *Fudan University, Shanghai 200443, People's Republic of China*

¹⁰ *G.I. Budker Institute of Nuclear Physics SB RAS (BINP), Novosibirsk 630090, Russia*

¹¹ *GSI Helmholtzcentre for Heavy Ion Research GmbH, D-64291 Darmstadt, Germany*

¹² *Guangxi Normal University, Guilin 541004, People's Republic of China*

¹³ *Guangxi University, Nanning 530004, People's Republic of China*

¹⁴ *Hangzhou Normal University, Hangzhou 310036, People's Republic of China*

¹⁵ *Helmholtz Institute Mainz, Johann-Joachim-Becher-Weg 45, D-55099 Mainz, Germany*

¹⁶ *Henan Normal University, Xinxiang 453007, People's Republic of China*

¹⁷ *Henan University of Science and Technology, Luoyang 471003, People's Republic of China*

¹⁸ *Huangshan College, Huangshan 245000, People's Republic of China*

¹⁹ *Hunan Normal University, Changsha 410081, People's Republic of China*

²⁰ *Hunan University, Changsha 410082, People's Republic of China*

²¹ *Indian Institute of Technology Madras, Chennai 600036, India*

²² *Indiana University, Bloomington, Indiana 47405, USA*

²³ *(A)INFN Laboratori Nazionali di Frascati, I-00044, Frascati, Italy; (B)INFN Sezione di Perugia, I-06100, Perugia, Italy; (C)University of Perugia, I-06100, Perugia, Italy*

²⁴ *(A)INFN Sezione di Ferrara, I-44122, Ferrara, Italy; (B)University of Ferrara, I-44122, Ferrara, Italy*

²⁵ *Institute of Modern Physics, Lanzhou 730000, People's Republic of China*

²⁶ *Institute of Physics and Technology, Peace Ave. 54B, Ulaanbaatar 13330, Mongolia*

²⁷ *Jilin University, Changchun 130012, People's Republic of China*

²⁸ *Johannes Gutenberg University of Mainz, Johann-Joachim-Becher-Weg 45, D-55099 Mainz, Germany*

²⁹ *Joint Institute for Nuclear Research, 141980 Dubna, Moscow region, Russia*

³⁰ *Justus-Liebig-Universitaet Giessen, II. Physikalisches Institut, Heinrich-Buff-Ring 16, D-35392 Giessen, Germany*

³¹ *KVI-CART, University of Groningen, NL-9747 AA Groningen, The Netherlands*

³² *Lanzhou University, Lanzhou 730000, People's Republic of China*

³³ *Liaoning Normal University, Dalian 116029, People's Republic of China*

³⁴ *Liaoning University, Shenyang 110036, People's Republic of China*

- ³⁵ Nanjing Normal University, Nanjing 210023, People's Republic of China
- ³⁶ Nanjing University, Nanjing 210093, People's Republic of China
- ³⁷ Nankai University, Tianjin 300071, People's Republic of China
- ³⁸ Peking University, Beijing 100871, People's Republic of China
- ³⁹ Qufu Normal University, Qufu 273165, People's Republic of China
- ⁴⁰ Shandong Normal University, Jinan 250014, People's Republic of China
- ⁴¹ Shandong University, Jinan 250100, People's Republic of China
- ⁴² Shanghai Jiao Tong University, Shanghai 200240, People's Republic of China
- ⁴³ Shanxi Normal University, Linfen 041004, People's Republic of China
- ⁴⁴ Shanxi University, Taiyuan 030006, People's Republic of China
- ⁴⁵ Sichuan University, Chengdu 610064, People's Republic of China
- ⁴⁶ Soochow University, Suzhou 215006, People's Republic of China
- ⁴⁷ Southeast University, Nanjing 211100, People's Republic of China
- ⁴⁸ State Key Laboratory of Particle Detection and Electronics,
Beijing 100049, Hefei 230026, People's Republic of China
- ⁴⁹ Sun Yat-Sen University, Guangzhou 510275, People's Republic of China
- ⁵⁰ Tsinghua University, Beijing 100084, People's Republic of China
- ⁵¹ (A)Ankara University, 06100 Tandogan, Ankara, Turkey; (B)Istanbul Bilgi
University, 34060 Eyup, Istanbul, Turkey; (C)Uludag University, 16059 Bursa,
Turkey; (D)Near East University, Nicosia, North Cyprus, Mersin 10, Turkey
- ⁵² University of Chinese Academy of Sciences, Beijing 100049, People's Republic of China
- ⁵³ University of Hawaii, Honolulu, Hawaii 96822, USA
- ⁵⁴ University of Jinan, Jinan 250022, People's Republic of China
- ⁵⁵ University of Manchester, Oxford Road, Manchester, M13 9PL, United Kingdom
- ⁵⁶ University of Minnesota, Minneapolis, Minnesota 55455, USA
- ⁵⁷ University of Muenster, Wilhelm-Klemm-Str. 9, 48149 Muenster, Germany
- ⁵⁸ University of Oxford, Keble Rd, Oxford, UK OX13RH
- ⁵⁹ University of Science and Technology Liaoning, Anshan 114051, People's Republic of China
- ⁶⁰ University of Science and Technology of China, Hefei 230026, People's Republic of China
- ⁶¹ University of South China, Hengyang 421001, People's Republic of China
- ⁶² University of the Punjab, Lahore-54590, Pakistan
- ⁶³ (A)University of Turin, I-10125, Turin, Italy; (B)University of Eastern
Piedmont, I-15121, Alessandria, Italy; (C)INFN, I-10125, Turin, Italy
- ⁶⁴ Uppsala University, Box 516, SE-75120 Uppsala, Sweden
- ⁶⁵ Wuhan University, Wuhan 430072, People's Republic of China
- ⁶⁶ Xinyang Normal University, Xinyang 464000, People's Republic of China
- ⁶⁷ Zhejiang University, Hangzhou 310027, People's Republic of China
- ⁶⁸ Zhengzhou University, Zhengzhou 450001, People's Republic of China
- ^a Also at Bogazici University, 34342 Istanbul, Turkey
- ^b Also at the Moscow Institute of Physics and Technology, Moscow 141700, Russia
- ^c Also at the Novosibirsk State University, Novosibirsk, 630090, Russia
- ^d Also at the NRC "Kurchatov Institute", PNPI, 188300, Gatchina, Russia
- ^e Also at Istanbul Arel University, 34295 Istanbul, Turkey
- ^f Also at Goethe University Frankfurt, 60323 Frankfurt am Main, Germany
- ^g Also at Key Laboratory for Particle Physics, Astrophysics and Cosmology, Ministry
of Education; Shanghai Key Laboratory for Particle Physics and Cosmology; Institute
of Nuclear and Particle Physics, Shanghai 200240, People's Republic of China
- ^h Also at Key Laboratory of Nuclear Physics and Ion-beam Application (MOE) and Institute
of Modern Physics, Fudan University, Shanghai 200443, People's Republic of China
- ⁱ Also at Harvard University, Department of Physics, Cambridge, MA, 02138, USA
- ^j Currently at: Institute of Physics and Technology, Peace Ave.54B, Ulaanbaatar 13330, Mongolia

^k Also at State Key Laboratory of Nuclear Physics and Technology,
Peking University, Beijing 100871, People's Republic of China

^l School of Physics and Electronics, Hunan University, Changsha 410082, China

Using 2.93 fb^{-1} of e^+e^- collision data collected at a center-of-mass energy of 3.773 GeV with the BESIII detector, the first observation of the doubly Cabibbo-suppressed decay $D^+ \rightarrow K^+\pi^+\pi^-\pi^0$ is reported. After removing decays that contain narrow intermediate resonances, including $D^+ \rightarrow K^+\eta$, $D^+ \rightarrow K^+\omega$, and $D^+ \rightarrow K^+\phi$, the branching fraction of the decay $D^+ \rightarrow K^+\pi^+\pi^-\pi^0$ is measured to be $(1.13 \pm 0.08_{\text{stat}} \pm 0.03_{\text{syst}}) \times 10^{-3}$. The ratio of branching fractions of $D^+ \rightarrow K^+\pi^+\pi^-\pi^0$ over $D^+ \rightarrow K^-\pi^+\pi^+\pi^0$ is found to be $(1.81 \pm 0.15)\%$, which corresponds to $(6.28 \pm 0.52) \tan^4 \theta_C$, where θ_C is the Cabibbo mixing angle. This ratio is significantly larger than the corresponding ratios for other doubly Cabibbo-suppressed decays. The asymmetry of the branching fractions of charge-conjugated decays $D^\pm \rightarrow K^\pm\pi^\pm\pi^\mp\pi^0$ is also determined, and no evidence for CP violation is found. In addition, the first evidence for the $D^+ \rightarrow K^+\omega$ decay, with a statistical significance of 3.3σ , is presented and the branching fraction is measured to be $\mathcal{B}(D^+ \rightarrow K^+\omega) = (5.7_{-2.1}^{+2.5}_{\text{stat}} \pm 0.2_{\text{syst}}) \times 10^{-5}$.

PACS numbers: 13.20.Fc, 14.40.Lb

Doubly Cabibbo-suppressed (DCS) decays of D mesons can provide unique insight into weak decay mechanisms of charmed hadrons. To date, DCS decays of charmed hadrons remain relatively unexplored [1]. The naive expectation for the DCS decay rate relative to its Cabibbo-favored (CF) counterpart [2, 3] is of the order $\tan^4 \theta_C \sim 0.29\%$, where θ_C is the Cabibbo mixing angle. The known ratios of DCS and CF decay rates [4] roughly support this expectation, with the exception of $D^+ \rightarrow K^-\pi^+\pi^+$ [5] where the ratio is doubled due to identical particles in the final state. A measurement of the branching fraction (BF) of $D^+ \rightarrow K^+\pi^+\pi^-\pi^0$ and a comparison with its CF counterpart provides a crucial test of this expectation.

In theory the BFs of $D \rightarrow VP$ decays, where V and P denote vector and pseudoscalar mesons, respectively, can be calculated after incorporating quark SU(3)-flavor symmetry and symmetry breaking as well as charge-parity (CP) violation [3, 6–13]. The experimental information on DCS $D \rightarrow VP$ decays is currently limited. Investigation of $D^+ \rightarrow K^+\pi^+\pi^-\pi^0$ offers an ideal opportunity to determine the BF of $D^+ \rightarrow K^+\omega$ with $\omega \rightarrow \pi^+\pi^-\pi^0$, where ω stands for $\omega(782)$ throughout this Letter. The result is important to improve our understanding of quark SU(3)-flavor symmetry and symmetry breaking and also benefits theoretical calculations of CP violation [3, 6–13].

In the Standard Model, CP violation in the weak decays of hadrons arises due to a single irreducible phase in the Cabibbo-Kobayashi-Maskawa matrix [14]. CP violation in charmed-hadron decays is expected to be small, up to a few 10^{-3} for singly Cabibbo-suppressed processes, and much smaller for CF and DCS processes [12, 15]. In the past two decades, CP violation

in charm sector has been extensively explored [16]. In 2019, the LHCb collaboration reported an observation of CP violation in the singly-Cabibbo-suppressed decays $D^0 \rightarrow K^+K^-$ and $D^0 \rightarrow \pi^+\pi^-$ [17]. Searching for CP violation in DCS decays offers complementary information about CP violation in the charm sector.

This Letter reports the first measurement of the absolute BFs of the DCS decays $D^+ \rightarrow K^+\pi^+\pi^-\pi^0$ and $D^+ \rightarrow K^+\omega$. Charge-conjugated decays are always implied unless stated otherwise. The CP asymmetry of $D^\pm \rightarrow K^\pm\pi^\pm\pi^\mp\pi^0$ is also presented.

This work is performed by using 2.93 fb^{-1} of e^+e^- collision data [18] collected with the BESIII detector at the center-of-mass energy of $\sqrt{s} = 3.773 \text{ GeV}$. This energy is near the resonance peak of the $\psi(3770)$, which predominantly decays into $D\bar{D}$ (D denotes D^0 or D^+) pair. The two D mesons are produced close to rest in the centre of mass frame without accompanying hadron(s), thereby offering ideal environment to study D meson decays with the double-tag (DT) technique, pioneered by the Mark III Collaboration [19].

Details about the design and performance of the BESIII detector are given in Refs. [20, 21]. Simulated samples produced with a GEANT4-based [22] Monte Carlo (MC) package, which includes the geometric description of the BESIII detector and the detector response, are used to determine the detection efficiency and to estimate backgrounds. The simulation includes the beam energy spread and initial state radiation (ISR) in the e^+e^- annihilations modeled with the generator KKMC [23]. The signal of $D^+ \rightarrow K^+\pi^+\pi^-\pi^0$ is simulated using an MC generator that incorporates the resonant decays $D^+ \rightarrow K^*(892)^0\rho(770)^+$, $K^*(892)^+\rho(770)^0$, $K^+\eta$, $K^+\omega$, the phase space decay $D^+ \rightarrow K^+\pi^+\pi^-\pi^0$, and possible interferences. The parameters of the generator have been tuned to reach a good data-MC agreement in distributions of the daughter particle momenta and the invariant masses of each two- and

* Corresponding authors:

xpan19@fudan.edu.cn, luot@fudan.edu.cn, mahl@ihep.ac.cn

three-body particle combinations. The signal of $D^+ \rightarrow K^+\omega$ is simulated using an MC generator which simulates pseudoscalar meson decays into vector meson and scalar meson [24]. The background is studied using an inclusive MC sample that consists of the production of $D\bar{D}$ pairs with consideration of quantum coherence for all neutral D modes, the non- $D\bar{D}$ decays of the $\psi(3770)$, the ISR production of the J/ψ and $\psi(3686)$ states, and the continuum processes incorporated in KKMC. The known decay modes are modeled with EVTGEN [24] using the known BFs taken from the Particle Data Group [1], while the remaining unknown decays from the charmonium states are modeled with LUNDCHARM [25]. Final state radiation from charged final state particles is incorporated with the PHOTOS package [26].

We obtain the BFs by reconstructing signal D^+ decays in events with D^- decays reconstructed in one of the three decay modes $D^- \rightarrow K^+\pi^-\pi^-$, $D^- \rightarrow K_S^0\pi^-$, and $D^- \rightarrow K^+\pi^-\pi^-\pi^0$. If a D^- meson is found, it is referred to as a single-tag (ST) candidate. An event in which a signal D^+ decay and an ST D^- are simultaneously found is referred as a double-tag event. The BF of the signal decay is given by

$$\mathcal{B}_{\text{sig}} = \frac{N_{\text{DT}}}{\sum_{i=1}^3 N_{\text{ST}}^i (\epsilon_{\text{DT}}^i / \epsilon_{\text{ST}}^i)}, \quad (1)$$

where N_{DT} is the number of events with any D^- tag and a signal candidate, ϵ_{DT}^i is the signal selection efficiency for an event with a D^- in the i -th tag mode, and N_{ST}^i and ϵ_{ST}^i are the number of tags and reconstruction efficiency for D^- candidates in mode i .

The K_S^0 and π^0 candidates are reconstructed via $K_S^0 \rightarrow \pi^+\pi^-$ and $\pi^0 \rightarrow \gamma\gamma$, respectively. For the reconstruction and identification of K^\pm , π^\pm , K_S^0 , and π^0 we use the same criteria as in Refs. [27–36]. The tagged D^- mesons are selected using two variables, the energy difference

$$\Delta E_{\text{tag}} \equiv E_{D^-} - E_b, \quad (2)$$

and the beam-constrained mass

$$M_{\text{BC}}^{\text{tag}} \equiv \sqrt{E_b^2 - |\vec{p}_{D^-}|^2}, \quad (3)$$

where E_b is the beam energy, and \vec{p}_{D^-} and E_{D^-} are the momentum and the energy of the D^- candidate in the e^+e^- rest frame. For each tag mode, if there are multiple combinations, the one giving the minimum $|\Delta E_{\text{tag}}|$ is retained for further analysis. The tagged D^- are required to satisfy $\Delta E_{\text{tag}} \in (-55, 40)$ MeV for the decay mode containing a π^0 , and $\Delta E_{\text{tag}} \in (-25, 25)$ MeV for the other decay modes. The yields of ST D^- mesons were obtained from maximum likelihood fits to the $M_{\text{BC}}^{\text{tag}}$ distributions of the accepted ST candidates [27–32]. The fit results are shown in Fig. 1. The total ST D^- yield is

$$N_{\text{ST}} = (1150.3 \pm 1.5_{\text{stat}}) \times 10^3.$$

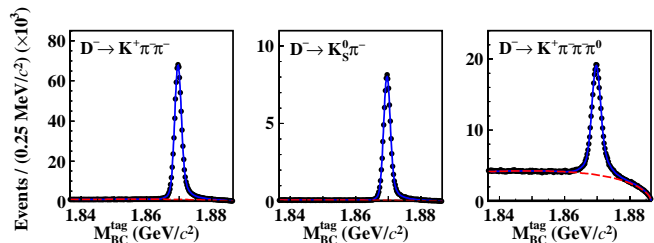


Fig. 1. Fits to the M_{BC} distributions of the ST D^- candidates. Data are shown as dots with error bars. The blue solid and red dashed curves are the fit results and the fitted backgrounds, respectively.

The signal D^+ candidates are reconstructed from the particles that have not been used for the tagged D^- reconstruction. They are identified using the energy difference and the beam-constrained mass of the signal side, ΔE_{sig} and $M_{\text{BC}}^{\text{sig}}$, calculated similarly to Eqs. (2) and (3), respectively, with D^- replaced by D^+ . If there are multiple combinations, caused mainly due to incorrectly π^0 , the one giving the minimum $|\Delta E_{\text{sig}}|$ is retained for further analysis. The signal side is required to be within $\Delta E_{\text{sig}} \in (-58, 45)$ MeV. The invariant mass of the $\pi^+\pi^-$ pair must satisfy the condition $|M_{\pi^+\pi^-} - M_{K_S^0}| > 20$ MeV/ c^2 to reject the dominant peaking background from the singly Cabibbo-suppressed decay $D^+ \rightarrow K_S^0 K^+\pi^0$. This requirement corresponds to about $\pm 5\sigma$ of the experimental resolution. To suppress non- D^+D^- events, the opening angle between the D^+ and D^- candidates is required to be greater than 160° , which results in a loss of 6% of the signal but rejects 34% of the background contributions. The top-left panel of Fig. 2 shows the $M_{\text{BC}}^{\text{tag}}$ vs. $M_{\text{BC}}^{\text{sig}}$ distribution of the accepted candidates for $D^+ \rightarrow K^+\pi^+\pi^-\pi^0$ in data. The comparison of two-body and three-body mass distributions of the accepted $D^+ \rightarrow K^+\pi^+\pi^-\pi^0$ candidate events can be found in the supplemental material [37].

Furthermore, the $D^+ \rightarrow K^+\omega$ candidates are selected from events with $\pi^+\pi^-\pi^0$ invariant mass within $|M_{\pi^+\pi^-\pi^0} - M_\omega| < 40$ MeV/ c^2 , where M_ω is the nominal mass of the ω meson [1]. This requirement is set by taking into account both the natural width of the ω meson and the invariant mass resolution. To suppress non- ω backgrounds, the ω helicity angle is required to satisfy $|\cos\theta_\omega| > 0.57$, where θ_ω is the opening angle between the normal to the $\omega \rightarrow \pi^+\pi^-\pi^0$ decay plane and the direction of the D^+ meson in the ω rest frame. Moreover, the normalized slope parameter $\lambda/\lambda_{\text{max}}$, introduced in Ref. [38], is required to be greater than 0.21, where the criterion is based on an optimization using the inclusive MC sample. The middle-left and bottom-left figures of Fig. 2 show the $M_{\text{BC}}^{\text{tag}}$ vs. $M_{\text{BC}}^{\text{sig}}$ distributions of the accepted candidates with the aforementioned additional

requirements for $D^+ \rightarrow K^+\pi^+\pi^-\pi^0$ in data, with $M_{\pi^+\pi^-\pi^0}$ in the ω signal region and the ω sideband region, defined as $M_{\pi^+\pi^-\pi^0} \in (0.60, 0.70) \cup (0.85, 0.95)$ GeV/ c^2 , respectively. Figure 3 shows the definitions of the ω signal and sideband regions.

In the $M_{\text{BC}}^{\text{tag}}$ vs. $M_{\text{BC}}^{\text{sig}}$ distributions, as shown in the left column of Fig. 2, signal events concentrate around $M_{\text{BC}}^{\text{tag}} = M_{\text{BC}}^{\text{sig}} = M_D$, where M_D is the nominal mass of the D^+ meson [1]. Background events are divided into three categories. The first (BKGI) is from events with correctly reconstructed D^+ (D^-) and incorrectly reconstructed D^- (D^+). This background is distributed along the horizontal and vertical bands. The second (BKGII) describes events found along the diagonal, which are mainly from the $e^+e^- \rightarrow q\bar{q}$ processes. The third (BKGIII) consists of uniformly distributed events in which both the tagged D^- and the signal D^+ are reconstructed incorrectly. For the decay $D^+ \rightarrow K^+\pi^+\pi^-\pi^0$ the peaking backgrounds from $D^+ \rightarrow K^+K^-(\rightarrow \pi^-\pi^0)\pi^+$ decays and from the residual $D^+ \rightarrow K_S^0(\rightarrow \pi^+\pi^-)K^+\pi^0$ events are evaluated using the MC simulations. For the decay $D^+ \rightarrow K^+\omega$, the peaking background contributions are dominated by the non- ω decays $D^+ \rightarrow K^+\pi^+\pi^-\pi^0$. This peaking background has the same event topology as the signal and is estimated using data events in the ω sideband region defined above.

To extract the DT yields, a two-dimensional (2D) unbinned maximum likelihood fit is performed on the corresponding $M_{\text{BC}}^{\text{tag}}$ vs. $M_{\text{BC}}^{\text{sig}}$ distribution. The 2D probability density function (PDF) for the signal is taken from the MC simulation. The PDFs of background contributions are constructed as [31, 34, 35, 39, 40]

- BKGI: $b(x) \cdot c_y(y; E_b, \xi_y) + b(y) \cdot c_x(x; E_b, \xi_x)$,
- BKGII: $c_z(z; \sqrt{2}E_b, \xi_z) \cdot g(k; 0, \sigma_k)$,
- BKGIII: $c_x(x; E_b, \xi_x) \cdot c_y(y; E_b, \xi_y)$.

Here, $x = M_{\text{BC}}^{\text{tag}}$, $y = M_{\text{BC}}^{\text{sig}}$, $z = (x + y)/\sqrt{2}$, and $k = (x - y)/\sqrt{2}$. The functions $b(x)$ and $b(y)$ are the one-dimensional signal shapes taken from the MC simulation. The function c_f is the ARGUS function [41] defined as

$$c_f(f; E_b, \xi_f) = A_f f \left(1 - \frac{f^2}{E_b^2}\right)^{\frac{1}{2}} e^{\xi_f \left(1 - \frac{f^2}{E_b^2}\right)}, \quad (4)$$

where f denotes x , y , or z , E_b is fixed at 1.8865 GeV, A_f is a normalization factor, and ξ_f is a fit parameter. The function $g(k; \sigma_k)$ is a Gaussian distribution with a mean of zero and a standard deviation $\sigma_k = \sigma_0 \cdot (\sqrt{2}E_b - z)^p$, where σ_0 and p are parameters determined by the fit. For the decay $D^+ \rightarrow K^+\pi^+\pi^-\pi^0$ the yields and shapes of the peaking background contributions are fixed to the expectation from the MC simulations. The BKGIII component is ignored due to limited data. All other parameters are left free.

To extract the signal yield of $D^+ \rightarrow K^+\omega$, simultaneous 2D fits are performed on the events in the ω signal and sideband regions. The background PDFs are fixed to the shapes obtained from the $D^+ \rightarrow K^+\pi^+\pi^-\pi^0$ fit. The ratio of the background yield in the ω sideband region and in the ω signal region is fixed to the value $f_\omega = 4.12 \pm 0.08$ obtained using the $D^+ \rightarrow K^+\pi^+\pi^-\pi^0$ MC simulation. The reliability of the choice and normalization of the nominal ω sideband region has been further verified by using those events with $M_{\pi^+\pi^-\pi^0} \in (0.85, 1.35)$ GeV/ c^2 arbitrarily. Both BKGI and BKGIII components are ignored in these two fits because of limited data.

The spectra in the middle and right columns in Fig. 2 show the projections on $M_{\text{BC}}^{\text{tag}}$ and $M_{\text{BC}}^{\text{sig}}$ of the 2D fits to data. For both signal decay modes the statistical significance is evaluated as $\sqrt{-2\ln(\mathcal{L}_0/\mathcal{L}_{\text{max}})}$, where \mathcal{L}_{max} is the maximum likelihood of the nominal fit and \mathcal{L}_0 is the likelihood of the fit excluding the signal PDF, and the degree of freedom is assumed to be 1. The statistical significance is found to be 23.3σ for $D^+ \rightarrow K^+\pi^+\pi^-\pi^0$ and 3.3σ for $D^+ \rightarrow K^+\omega$. For $D^+ \rightarrow K^+\omega$, the effect of the fluctuation of the ω sideband events has been considered in the simultaneous fit.

The numbers of N_{DT} and ϵ_{sig} as well as the obtained BFs of the two decays are summarized in the first two rows of Table 1.

With the DT method, most of the uncertainties related to the ST selection are negligible. The systematic uncertainties arise from the following sources and are estimated relative to the measured BFs. The uncertainty on the total ST D^- yield is due to the fit to the $M_{\text{BC}}^{\text{tag}}$ distributions and is estimated to be 0.5% [27–29]. The tracking and PID efficiencies of K^\pm and π^\pm are studied with DT $D\bar{D}$ hadronic events. A small difference between the K^\pm tracking efficiency in data and in MC simulation is found, but those for the efficiencies of K^\pm PID, π^\pm tracking and π^\pm PID are negligible. The averaged data-MC difference of K^\pm tracking efficiency weighted by the momentum spectrum of signal MC events is 1.8%. After correcting the MC efficiencies by this averaged data-MC difference, the systematic uncertainties of tracking efficiencies are estimated to be 0.3% per K^\pm or π^\pm . The systematic uncertainties originating from PID efficiencies are assigned as 0.3% per K^\pm or π^\pm . The efficiency of reconstructing a π^0 meson is investigated by using the DT $D\bar{D}$ hadronic decay samples of $D^0 \rightarrow K^-\pi^+$, $K^-\pi^+\pi^+\pi^-$ vs. $\bar{D}^0 \rightarrow K^+\pi^-\pi^0$, $K_S^0\pi^0$ [27, 28]. The averaged data-MC difference of the π^0 reconstruction efficiencies, weighted by the momentum spectra of signal MC events, is 0.7% per π^0 . After correcting the MC efficiencies by this averaged data-MC difference the systematic uncertainty arising from π^0 reconstruction is estimated as 0.8% per π^0 . The uncertainties of the quoted BFs of $\omega \rightarrow \pi^+\pi^-\pi^0$ and $\pi^0 \rightarrow \gamma\gamma$ decays are 0.8% and 0.03% [1], respectively.

Table 1. The ST and DT yields in data (N_{ST} and N_{DT}), the signal efficiencies (ϵ_{sig}), and the obtained BF's before (\mathcal{B}_{sig}) and after ($\mathcal{B}_{\text{sig}}^*$) removing the contribution from $D^+ \rightarrow K^+\eta$, $K^+\omega$, and $K^+\phi$ [42]. Here, we ignore the possible interferences between these two-body decays and the other processes in $D^+ \rightarrow K^+\pi^+\pi^-\pi^0$. The uncertainties are statistical only.

Decay mode	$N_{\text{ST}} (\times 10^3)$	N_{DT}	$\epsilon_{\text{sig}} (\%)$	$\mathcal{B}_{\text{sig}} (\times 10^{-3})$	$\mathcal{B}_{\text{sig}}^* (\times 10^{-3})$
$D^\pm \rightarrow K^\pm \pi^\pm \pi^\mp \pi^0$	1150.3 ± 1.5	350 ± 22	25.03 ± 0.13	1.21 ± 0.08	1.13 ± 0.08
$D^\pm \rightarrow K^\pm \omega$	1150.3 ± 1.5	$9.2^{+4.0}_{-3.4}$	14.14 ± 0.09	$(5.7^{+2.5}_{-2.1}) \times 10^{-2}$	-
$D^+ \rightarrow K^+ \pi^+ \pi^- \pi^0$	573.5 ± 1.0	181 ± 15	25.20 ± 0.18	1.25 ± 0.11	1.17 ± 0.11
$D^- \rightarrow K^- \pi^- \pi^+ \pi^0$	572.7 ± 1.0	165 ± 15	24.95 ± 0.18	1.16 ± 0.11	1.08 ± 0.11

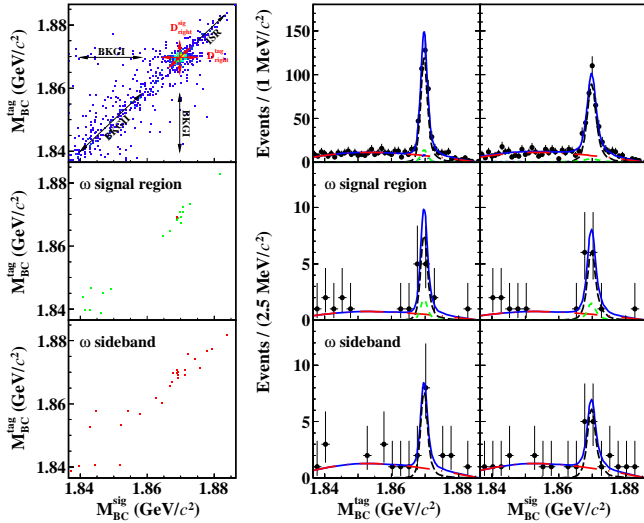


Fig. 2. Distributions of (left column) $M_{\text{BC}}^{\text{tag}}$ vs. $M_{\text{BC}}^{\text{sig}}$, and the projections of the corresponding 2D fits on (middle column) $M_{\text{BC}}^{\text{tag}}$ and (right column) $M_{\text{BC}}^{\text{sig}}$, for the DT candidate events of $D^- \rightarrow$ all tags vs. $D^+ \rightarrow K^+\pi^+\pi^-\pi^0$. The top, middle, and bottom rows correspond to all events, events lying in ω signal region, and those falling in ω sideband region, respectively. In the figures of the middle and right columns, data are shown as dots with error bars; the blue solid, black dashed, blue dot-dashed, red dot-long-dashed, and green dashed curves denote the overall fit results, signal, BKG I, BKG II, and peaking background components, respectively.

To estimate the systematic uncertainty from the 2D fit, the measurements are repeated by varying the signal shape, the endpoint of the ARGUS function, and the fixed number of peaking background events (by varying $\pm 1\sigma$ of the quoted BF's of the dominant peaking backgrounds of $D^+ \rightarrow K_S^0(\rightarrow \pi^+\pi^-)K^+\pi^0$ and $D^+ \rightarrow K^+K^-(\rightarrow \pi^-\pi^0)\pi^+$). Quadratically summing over the changes of the BF's gives the systematic uncertainties, which are 0.9% for $D^+ \rightarrow K^+\pi^+\pi^-\pi^0$ and negligible for $D^+ \rightarrow K^+\omega$. The systematic uncertainty related to the D^+D^- opening angle requirement is assigned as 0.5% based on DT events where the signal decays are replaced by the CF $D^+ \rightarrow K^-\pi^+\pi^+\pi^0$ channel. The systematic uncertainty associated with the ΔE_{sig} requirement is evaluated to be 0.2%, estimated by smearing the ΔE_{sig}

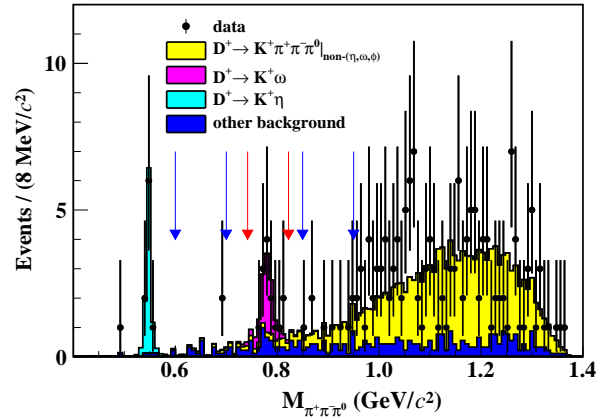


Fig. 3. Distribution of $M_{\pi^+\pi^-\pi^0}$ for $D^+ \rightarrow K^+\pi^+\pi^-\pi^0$ candidates in data (dots with error bars). Histograms in yellow, pink, and cyan are the signal MC events of $D^+ \rightarrow K^+\pi^+\pi^-\pi^0|_{\text{non-}\eta,\omega,\phi}$, $D^+ \rightarrow K^+\omega$, and $D^+ \rightarrow K^+\eta$ normalized with individual BF's and efficiencies, and blue histogram is the background estimated using the inclusive MC sample, scaled to the rest event yield in data. Events have been selected using $M_{\text{BC}}^{\text{tag}(\text{sig})} \in (1.863, 1.875) \text{ GeV}/c^2$ and all other requirements for $D^+ \rightarrow K^+\omega$ except for the ω signal mass window. The red arrows denote the ω signal region. The blue arrows denote the ω sideband regions.

distribution for signal MC events. The systematic uncertainty due to K_S^0 rejection is negligible since the mass resolution is well reproduced by the MC simulation. The boundaries of the ω sideband regions were varied by $\pm 5 \text{ MeV}/c^2$ and the corresponding uncertainty was found to be negligible. The limited number of simulated events contributes 0.5% uncertainty for $D^+ \rightarrow K^+\pi^+\pi^-\pi^0$ and 0.6% for $D^+ \rightarrow K^+\omega$. The systematic uncertainty related to the MC modeling for $D^+ \rightarrow K^+\pi^+\pi^-\pi^0$ is assigned to be 1.3%, which is the difference of the DT efficiencies with and without involving the less significant decays of $D^+ \rightarrow K^+\eta$, $K^+\omega$, and $K^+\phi$, and the effects of high excited states are negligible. For $D^+ \rightarrow K^+\omega$, the systematic uncertainties of the MC modeling are mainly from the imperfect simulations on $\cos\theta_\omega$ and $\lambda/\lambda_{\text{max}}$. They are estimated using the DT events $D^0 \rightarrow K_S^0\omega$ vs. $\bar{D}^0 \rightarrow K^+\pi^-$, $K^+\pi^-\pi^0$, and $K^+\pi^-\pi^+\pi^+$. The

differences of the acceptance efficiencies of the $\cos\theta_\omega$ and λ/λ_{\max} requirements between data and MC simulations, 3.0% and 1.2%, are assigned as the corresponding systematic uncertainties, respectively. The uncertainty on the scale factor $f_\omega^{\text{sid}/\text{sig}}$ results in 0.6% uncertainty on the $D^+ \rightarrow K^+\omega$ signal.

The total systematic uncertainty of the BF measurement is 2.3% for $D^+ \rightarrow K^+\pi^+\pi^-\pi^0$ and 3.8% for $D^+ \rightarrow K^+\omega$, obtained by adding the above effects quadratically.

The BFs of the charge-conjugated decays $D^+ \rightarrow K^+\pi^+\pi^-\pi^0$ and $D^- \rightarrow K^-\pi^-\pi^+\pi^0$, $\mathcal{B}_{D^+\rightarrow K^+\pi^+\pi^-\pi^0}$ and $\mathcal{B}_{D^-\rightarrow K^-\pi^-\pi^+\pi^0}$, are measured separately. The asymmetry of these two BFs is determined as

$$\mathcal{A}_{CP}^{D^\pm \rightarrow K^\pm \pi^\pm \pi^\mp \pi^0} = \frac{\mathcal{B}_{D^+ \rightarrow K^+ \pi^+ \pi^- \pi^0} - \mathcal{B}_{D^- \rightarrow K^- \pi^- \pi^+ \pi^0}}{\mathcal{B}_{D^+ \rightarrow K^+ \pi^+ \pi^- \pi^0} + \mathcal{B}_{D^- \rightarrow K^- \pi^- \pi^+ \pi^0}}. \quad (5)$$

The corresponding ST yields, DT yields, signal efficiencies, and the obtained BFs are summarized in the last two rows of Table 1. The asymmetry is determined to be $\mathcal{A}_{CP}^{D^\pm \rightarrow K^\pm \pi^\pm \pi^\mp \pi^0} = (-0.04 \pm 0.06_{\text{stat}} \pm 0.01_{\text{syst}})$, where the systematic uncertainties of tracking and PID of the $\pi^+\pi^-$ pair, π^0 reconstruction, quoted BFs, and MC modeling cancel. Other systematic uncertainties are estimated separately as above. No evidence for CP violation is found.

In summary, using 2.93 fb^{-1} of data taken at $\sqrt{s} = 3.773 \text{ GeV}$ with the BESIII detector, the first observation and BF measurement of the DCS decay $D^+ \rightarrow K^+\pi^+\pi^-\pi^0$ are presented. Removing the contribution of the known decays $D^+ \rightarrow K^+\eta$, $K^+\omega$, and $K^+\phi$ [42] and ignoring the possible interferences between these decays and the other processes in $D^+ \rightarrow K^+\pi^+\pi^-\pi^0$, we obtain $\mathcal{B}_{D^+ \rightarrow K^+\pi^+\pi^-\pi^0}^* = (1.13 \pm 0.08_{\text{stat}} \pm 0.03_{\text{syst}}) \times 10^{-3}$, which is the largest among all known DCS decays in the charm sector. The evidence for the decay $D^+ \rightarrow K^+\omega$ is found and its BF is measured to be $(5.7^{+2.5}_{-2.1_{\text{stat}}} \pm 0.2_{\text{syst}}) \times 10^{-5}$. This BF is consistent with theoretical predictions that incorporate quark SU(3)-flavor symmetry and symmetry breaking [8], but disfavors predictions based on quark SU(3)-flavor symmetry without symmetry breaking [3, 9] and predictions based on the pole model [43] by $1.8\text{--}2.8\sigma$. This result will benefit future calculations of CP violation in the charm sector [3, 6–14].

The ratio of our result $\mathcal{B}_{D^+ \rightarrow K^+\pi^+\pi^-\pi^0}^*$ over the world averaged value of $\mathcal{B}_{D^+ \rightarrow K^-\pi^+\pi^+\pi^0}$ is $(1.81 \pm 0.15)\%$, corresponding to $(6.28 \pm 0.52) \tan^4 \theta_C$, where $\sin \theta_C = 0.2257$ [1]. This ratio is significantly larger than the values $(0.21\text{--}0.58)\%$ measured for the other DCS decays, $D^0 \rightarrow K^+\pi^-$, $D^0 \rightarrow K^+\pi^-\pi^-\pi^+$, $D^0 \rightarrow K^+\pi^-\pi^0$, $D^+ \rightarrow K^+\pi^+\pi^-$, $D_s^+ \rightarrow K^+K^+\pi^-$, and $\Lambda_c^+ \rightarrow pK^+\pi^-$ [1]. It is already known that the ratio of $\mathcal{B}_{D^0 \rightarrow K^+\pi^-\pi^-\pi^+} / \mathcal{B}_{D^0 \rightarrow K^-\pi^+\pi^+\pi^-}$ roughly supports $\tan^4 \theta_C$ [1]. This unexpected ratio implies that there is a massive isospin symmetry violation in the decays

$D^+ \rightarrow K^+\pi^+\pi^-\pi^0$ and $D^0 \rightarrow K^+\pi^-\pi^-\pi^+$, which may be caused by final state interactions and very different resonance structures in these two decays. Amplitude analyses of these decays with larger data samples [21] will provide crucial information to understand the origin of the anomalously large ratio. The asymmetry of the BFs of charge-conjugated decays $D^\pm \rightarrow K^\pm \pi^\pm \pi^\mp \pi^0$ is determined, and no evidence for CP violation is found.

The authors thank Prof. Fu-Sheng Yu for helpful discussions. The BESIII collaboration thanks the staff of BEPCII and the IHEP computing center for their strong support. This work is supported in part by National Key Basic Research Program of China under Contract No. 2015CB856700; National Natural Science Foundation of China (NSFC) under Contracts Nos. 11805037, 11775230, 11625523, 11635010, 11735014, 11822506, 11835012, 11935015, 11935016, 11935018, 11961141012; the Chinese Academy of Sciences (CAS) Large-Scale Scientific Facility Program; Joint Large-Scale Scientific Facility Funds of the NSFC and CAS under Contracts Nos. U1832121, U1732263, U1832207; CAS Key Research Program of Frontier Sciences under Contracts Nos. QYZDJ-SSW-SLH003, QYZDJ-SSW-SLH040; 100 Talents Program of CAS; INPAC and Shanghai Key Laboratory for Particle Physics and Cosmology; ERC under Contract No. 758462; German Research Foundation DFG under Contracts Nos. Collaborative Research Center CRC 1044, FOR 2359, FOR 2359, GRK 214; Istituto Nazionale di Fisica Nucleare, Italy; Ministry of Development of Turkey under Contract No. DPT2006K-120470; National Science and Technology fund; Olle Engkvist Foundation under Contract No. 200-0605; STFC (United Kingdom); The Knut and Alice Wallenberg Foundation (Sweden) under Contract No. 2016.0157; The Royal Society, UK under Contracts Nos. DH140054, DH160214; The Swedish Research Council; U. S. Department of Energy under Contracts Nos. DE-FG02-05ER41374, DE-SC-0012069.

-
- [1] P. A. Zyla *et al.* (Particle Data Group), *Prog. Theor. Exp. Phys.* **2020**, 083C01 (2020).
 - [2] H. J. Lipkin, *Nucl. Phys. Suppl.* **115**, 117 (2003).
 - [3] H. Y. Cheng and C. W. Chiang, *Phys. Rev. D* **81**, 074021 (2010).
 - [4] M. Artuso *et al.* (CLEO Collaboration), *Phys. Rev. D* **77**, 092003 (2008).
 - [5] B. R. Koet *et al.* (Belle Collaboration), *Phys. Rev. Lett.* **102**, 221802 (2009).
 - [6] Z. Z. Xing, *Mod. Phys. Lett. A* **34**, 1950238 (2019).
 - [7] H. J. Lipkin, *Phys. Rev. Lett.* **46**, 1307 (1981).
 - [8] Q. Qin, H. N. Li, C. D. Lü, and F. S. Yu, *Phys. Rev. D* **89**, 054006 (2014).
 - [9] H. Y. Cheng, C. W. Chiang, and A. L. Kuo, *Phys. Rev. D* **93**, 114010 (2016).
 - [10] W. Kwong and S. P. Rosen,

- Phys. Lett. B **298**, 413 (1993).
- [11] Y. Grossman and D. J. Robinson, *J. High Energy Phys.* **1304**, 067 (2013).
- [12] H. N. Li, C. D. Lü, and F. S. Yu, *Phys. Rev. D* **86**, 036012 (2012).
- [13] M. Saur and F. S. Yu, arXiv:2002.12088.
- [14] M. Kobayashi and T. Maskawa, *Prog. Theor. Phys.* **49**, 652 (1973).
- [15] H. Y. Cheng and C. W. Chiang, *Phys. Rev. D* **86**, 014014 (2012).
- [16] Y. Amhis *et al.* (Heavy Flavor Averaging Group), arXiv:1412.7515.
- [17] R. Aaij *et al.* (LHCb Collaboration), *Phys. Rev. Lett.* **122**, 211803 (2019).
- [18] M. Ablikim *et al.* (BESIII Collaboration), *Chin. Phys. C* **37**, 123001 (2013); *Phys. Lett. B* **753**, 629 (2016).
- [19] R. M. Baltrusaitis *et al.* (MARK III Collaboration), *Phys. Rev. Lett.* **56**, 2140 (1986); J. Adler *et al.* (MARK III Collaboration), *Phys. Rev. Lett.* **60**, 89 (1988);
- [20] M. Ablikim *et al.* (BESIII Collaboration), *Nucl. Instrum. Meth. A* **614**, 345 (2010).
- [21] M. Ablikim *et al.* (BESIII Collaboration), *Chin. Phys. C* **44**, 040001 (2020).
- [22] S. Agostinelli *et al.* (GEANT4 Collaboration), *Nucl. Instrum. Meth. A* **506**, 250 (2003).
- [23] S. Jadach, B. F. L. Ward, and Z. Was, *Phys. Rev. D* **63**, 113009 (2001); *Comput. Phys. Commun.* **130**, 260 (2000).
- [24] D. J. Lange, *Nucl. Instrum. Meth. A* **462**, 152 (2001); R. G. Ping, *Chin. Phys. C* **32**, 599 (2008).
- [25] J. C. Chen, G. S. Huang, X. R. Qi, D. H. Zhang, and Y. S. Zhu, *Phys. Rev. D* **62**, 034003 (2000).
- [26] E. Richter-Was, *Phys. Lett. B* **303**, 163 (1993).
- [27] M. Ablikim *et al.* (BESIII Collaboration), *Eur. Phys. J. C* **76**, 369 (2016).
- [28] M. Ablikim *et al.* (BESIII Collaboration), *Chin. Phys. C* **40**, 113001 (2016).
- [29] M. Ablikim *et al.* (BESIII Collaboration), *Phys. Rev. Lett.* **121**, 171803 (2018).
- [30] M. Ablikim *et al.* (BESIII Collaboration), *Phys. Rev. Lett.* **123**, 231801 (2019).
- [31] M. Ablikim *et al.* (BESIII Collaboration), *Phys. Rev. D* **101**, 052009 (2020).
- [32] M. Ablikim *et al.* (BESIII Collaboration), *Phys. Rev. D* **101**, 072005 (2020).
- [33] M. Ablikim *et al.* (BESIII Collaboration), *Phys. Rev. Lett.* **124**, 231801 (2020).
- [34] M. Ablikim *et al.* (BESIII Collaboration), *Phys. Rev. Lett.* **124**, 241803 (2020).
- [35] M. Ablikim *et al.* (BESIII Collaboration), arXiv:2007.10563.
- [36] M. Ablikim *et al.* (BESIII Collaboration), arXiv:2008.05754.
- [37] See Supplemental Material at the link (to be added by editor) for comparison of two-body and three-body mass distributions of the $D^+ \rightarrow K^+\pi^+\pi^-\pi^0$ candidate events between data and inclusive MC sample.
- [38] M. Ablikim *et al.* (BESIII Collaboration), *Phys. Rev. D* **100**, 052012 (2019).
- [39] M. Ablikim *et al.* (BESIII Collaboration), *Chin. Phys. C* **42**, 083001 (2018).
- [40] *Phys. Rev. D* **76**, 112001 (2007).
- [41] H. Albrecht *et al.* (ARGUS Collaboration), *Phys. Lett. B* **241**, 278 (1990).
- [42] This contribution is calculated by $\sum_{\mathcal{R}=1}^3 [\mathcal{B}(D^+ \rightarrow K^+\mathcal{R}) \cdot \mathcal{B}(\mathcal{R} \rightarrow \pi^+\pi^-\pi^0)]$, where \mathcal{R} sums over η , ω , and ϕ , $\mathcal{B}(D^+ \rightarrow K^+\omega)$ is obtained in this work, and the other BF's are quoted from the PDG [1].
- [43] F. S. Yu, X. X. Wang, and C. D. Lü *Phys. Rev. D* **84**, 074019 (2011).